

Modelling of the ice-edge failure process with curved failure surfaces

PENTTI KUJALA

Helsinki University of Technology, Ship Laboratory, Otakaari 4, SF-02150 Espoo, Finland

ABSTRACT. The failure process of a wedge-shaped ice edge is modelled by dividing the process in crushing failures at the contact and flaking failures initiating from high pressure in the contact. This type of approach has been shown earlier by Daley to give an explanation of the physical background of the line-like contact observed in ice-crushing tests and in full-scale measurements. Daley's model is developed further by studying the stress field in ice in more detail when applying the Coulomb macroscopic failure criterion to determine the force required for flaking failures. The analysis indicates that the shape of the flaking failure surface to minimise the force required to cause failure follows a logarithmic spiral. The shape of the spiral is related to the inner friction angle of ice and to the geometry of the ice edge. The curved flaking surfaces require considerably less force than straight surfaces used previously, especially with wide wedge angles. Finally, the model developed is used to simulate the time history of a crushing force measured in laboratory crushing tests and a good correspondence is obtained.

INTRODUCTION

Theoretical modelling of loads induced by ice impinging on structures requires analysis of the failure process of ice, a process initiated by contact between the structure and the ice. The contact creates a stress field in the ice, which causes failure in the ice once a critical stress level is reached. The behaviour of this local contact zone is the topic discussed in this paper.

The failure of ice under compression includes such phenomena as yielding, cracking, faulting, splitting and spalling. Also the word crushing is used, which can include all of the phenomena stated above. Ice before the failure can show a range of behaviour such as elastic, microcracking, viscoelastic and plastic. Complexity of the compression failure has resulted in various approaches to studying the failure process.

This paper develops a tool for studying the process of ice failure at the contact zone, so that the forces generated during this process can be used to study the behaviour of ice cover when, for example, moving ice hits a structure like a ship in compressive ice. A preliminary version of this kind of failure process analysis is given in Kujala and others (1993). That approach relies on observations made in laboratory ice-crushing tests (Joensuu and Riska, 1989; Fransson and others, 1991; Tuhkuri, 1993) and on full-scale observations on board an icebreaker (Riska and others, 1990), which have indicated that the contact between a structure and ice is linear. The theoretical failure-process model developed by Daley (1991) is applied, because it gives an explanation for the physical background of the linear contact. Daley's model includes a crushing region at the contact, and the high pressure in

this contact initiates shear flakes in the ice. The angle of the flakes is determined by applying a Coulomb failure criterion and calculating critical values for the gross stresses on various failure planes. Both the full-scale and laboratory test observations indicate, however, that the surface of the damaged ice is curved. Therefore in this paper Daley's model is developed further by studying the stress field in the ice edge in more detail.

The contact is assumed to be wide relative to the ice thickness. The model developed is two-dimensional and ice is considered as isotropic material.

MODELLING OF ICE FAILURE PROCESS IN COMPRESSION

General description of the model

In this section the basic principles of the approach and mathematical formulations required for modelling of the ice failure process in compression are presented. The flaking process is here defined using curved surfaces, which can be compared to spalling failures as defined by Kendall (1978) for cracks growing parallel to the ice surface until eventually emerging to the surface to remove a chip. The fracture mechanics approach for spalling created by Kendall and applied for ice by Wierzbicki (1985) assumes that a long crack due to axial splitting exists in ice and the criterion for the propagation of the crack defines the compressive strength of ice. The practical application of the theory is difficult, because no criteria are given for the forces required to run the cracks which initiate propagation. Therefore another

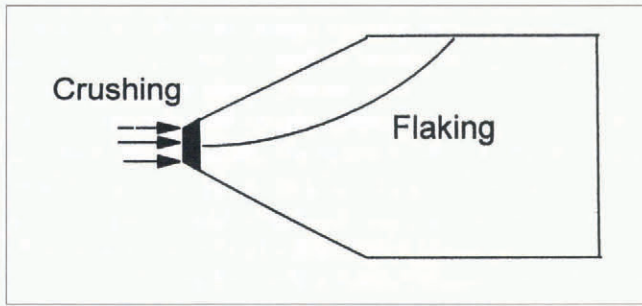


Fig. 1. Division of the failure process into crushing and flaking.

approach is chosen to evaluate the criterion for flaking.

It is assumed that the ice failure begins with crushing, and continues by flaking when the force in the contact zone is high enough for a slip surface to develop from the crushing region to the ice surface (Fig. 1). Slip surfaces are widely used in soil mechanics (e.g. Jaeger and Cook, 1979). The slip-surface approach is based on the assumption that the material is in a state of failure only along the slip surface, and the material outside this region behaves elastically. The criteria used for crushing and spalling are defined below.

The crushing zone

The linear contact height is typically some mm and contact pressures are in the range 20–30 MPa measured with 20 × 20 mm PVDF sensors (Joensuu and Riska, 1989). The rise time for the measured pressures is about 0.1 s at a crushing speed of 50 mm s⁻¹. Assuming that the stress in the ice is locally the same as the measured pressure, a figure of 300 MPa s⁻¹ is obtained for the maximum stress rate. Taking the elastic modulus $E = 7000 \text{ MPa}$ (Varsta, 1983) a strain rate $\epsilon = 4 \times 10^{-2}$ is reached in ice near the contact. Examination of the ice specimen after the crushing tests has revealed very

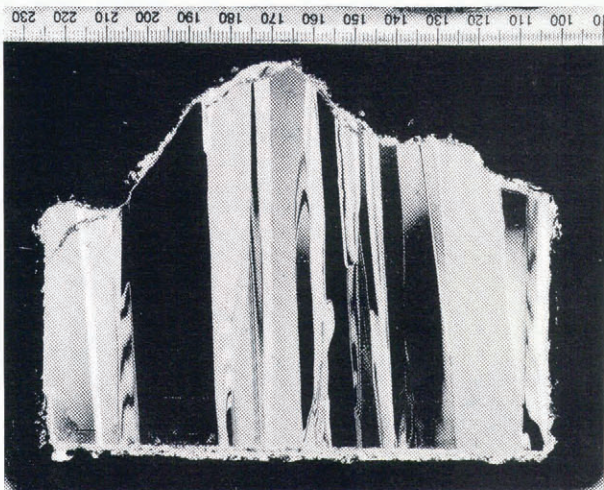


Fig. 2. A thin section of ice specimen after crushing tests with wedge-shaped S2 ice: wedge angle of 120° and ice thickness of 120 mm, crushing speed 50 m s⁻¹ (Tuhkuri, 1993).

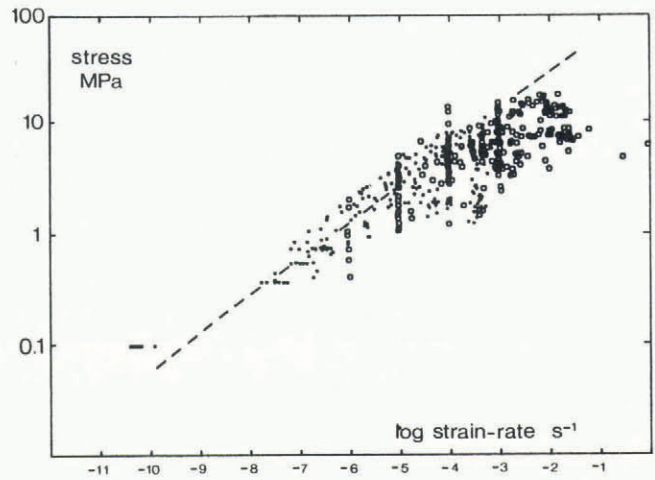


Fig. 3. Uniaxial horizontal compressive strength versus strain rate for columnar S2 ice normalised to zero brine volume and $T = -10^\circ\text{C}$ (Sanderson, 1988). Dotted line calculated with Equation (1).

little internal damage in the ice (Fig. 2) (Tuhkuri, 1993). Only a few cracks starting from the contact surface can be seen.

The physical background for the high pressures at the contact has not been properly clarified. High pressure can be caused by phenomena such as size effect, confinement, strain rate or pressure melting. It is generally known that decrease in specimen size increases the strength of the material due to the Weibull effect. Kendall (1978) has shown also with test specimens of polystyrene how axial splitting can change to crushing of the material with smaller specimens. Crushing results in much higher compressive strength values than axial splitting, because the cracks do not propagate; instead gross failure of the specimen occurs. Using ice material properties this transition from splitting to crushing can be estimated to take place with a specimen size of a few mm (Wierzbicki and Karr, 1988; Fransson and others, 1991). The effect of confinement on compressive strength has been clearly observed in the confined compressive strength. Increase of confinement during compressive strength tests of ice changes the failure mode from axial splitting to shear faulting, and finally to explosive fracture (Ashby and Hallam, 1986).

The strength of ice is very sensitive to loading rate, and increases with increasing strain rates. Sanderson (1988) has shown how the power-law creep curve follows measured maximum uniaxial compressive stresses up to strain rates of 10⁻³ s⁻¹ (Fig. 3).

The line given in Figure 3 to describe the maximum measured uniaxial compressive strength values in MPa for columnar S2 ice as a function of strain rate can be formulated:

$$\sigma_c = k\dot{\epsilon}_c^{1/3} \quad (1)$$

where k is a coefficient related to the temperature, T , so that with $T = -5^\circ\text{C}$, $k = 110$ and $T = -10^\circ\text{C}$, $k = 132$. The equation is crude, because it assumes that all ice deformations are viscous creep. It gives, however, a reasonable estimate for crushing pressures on the contact

line as using the strain rate $\epsilon = 4 \times 10^{-2} \text{ s}^{-1}$, a value $\sigma_c = 38 \text{ MPa}$ is obtained with $T = -5^\circ\text{C}$, which is close to the measured maximum pressures with the PVDF sensors in the tests of Joensuu and Riska (1989). The same equation was applied also by Fransson and others (1991) to explain high pressures on the contact line. The effect of strain rate on ice compressive strength with high confinement and small contact size is poorly known.

The high pressures observed in the contact zone have initiated a number of studies related to the pressure melting of ice (Gagnon and Sinha, 1991). No perfectly clear evidence of pressure melting has emerged. This can, however, be considered as the upper limit for possible contact pressures. It can be estimated with the formula (Hobbs, 1974, p. 61; Hallam and Nadreau, 1988):

$$p_c = 11|T|^{0.95} \tag{2}$$

where p_c is in MPa and T in $^\circ\text{C}$ giving a value $p_c = 50.7 \text{ MPa}$ with $T = -5^\circ\text{C}$. Equation (2) is valid in the range $0 > T > -22^\circ\text{C}$.

The most promising approach for calculating crushing pressure is to use Equation (1), even though it is strictly applicable only below strain rates of 10^{-3} s^{-1} as shown in Figure 3. The difference between measured strength values and those given by Equation (1) with higher strain rates is called the power-law breakdown: it is usually explained as due to the change of failure process and increase of brittle fracturing of the test specimen, thus lowering the compressive strength values measured. Following the arguments given by Kendall (1978) of the effect of contact height on the failure process and the small amount of cracking shown in Figure 2, it is possible to conclude that the narrow linear contact decreases the amount of cracking of ice thus extending the applicability of Equation (1) to higher strain rates. Consequently Equation (1), with Equation (2) specifying the upper limit, are considered at the present stage as the most adequate way to calculate pressure on the crushing zone.

The curved flaking process

The macroscopic failure criterion

The criterion for ice failure is determined using failure envelopes, which define the relationship between various stress components required to initiate failure. The complicated nature of compression failure of ice, as reviewed above, has also initiated a number of approaches to developing the failure envelope.

Observations in conducting compressive strength tests of ice have shown that the failure of ice under compression begins with development of microcracks, and continues with their propagation. Consequently research has concentrated on studies that include the cracking process in the failure criteria. The physical modelling of the failure process under compression concentrates on the effect of confinement on crack propagation and especially on the frictional sliding process of inclined cracks (wing-cracking) (Nemat-Nasser and Horii, 1982; Ashby and Hallam, 1986; Schulson, 1990; Schulson and Smith, 1992).

The idea of the frictional sliding model is that, out of plane, extensions or wings form within the tensile zone of

inclined microcracks and then grow along the direction of loading through frictional sliding across opposite faces of the parent crack. This model explains the effect of confinement as an increase in friction between crack surfaces due to the closing of cracks. With low and moderate confinement failure envelopes have been observed to follow the Coulomb failure criterion as shown by Schulson and Smith (1992) for columnar S2 ice. The relationship between the confined wing-cracking process and Coulomb failure criterion, discussed by Daley (1991), is briefly summarised in the following.

According to Coulomb failure criteria, shear failure on the plane occurs when (Jaeger and Cook, 1979):

$$|\tau_s| = S_i + \tan(\phi)\sigma_s \tag{3}$$

where σ_s and τ_s are normal and shear stresses across the plane, S_i is material constant which can be regarded as inherent shear strength of the material, $\tan(\phi)$ is the coefficient of internal friction of the material and ϕ is the angle of internal friction. Based on the wing-crack propagation failure criterion of Ashby and Hallam (1986), Daley (1991) has shown that material constants can be obtained from the relationships:

$$\sin(\phi) = 0.47\mu + 0.53 \tag{4}$$

$$S_i = 1.06S_c \sqrt{\frac{1-\mu}{\mu+3.25}} \tag{5}$$

where μ is an ice-ice friction factor and S_c is the uniaxial brittle compressive strength of ice. It can be obtained for example from the formula (Schulson, 1990):

$$S_c = \frac{Z_s K_{IC}}{(1-\mu)\sqrt{d}} \tag{6}$$

where K_{IC} is fracture toughness and d is the grain diameter of ice. The factor Z_s is a constant, which depends on the failure mode ($Z_s = 2.5$ for shear faulting and $Z_s = 1.8$ for axial splitting). These equations are used in this paper to evaluate the material parameters required for application of the Coulomb failure criterion.

Criterion for flaking

For determination of the flaking criterion, a wedge-

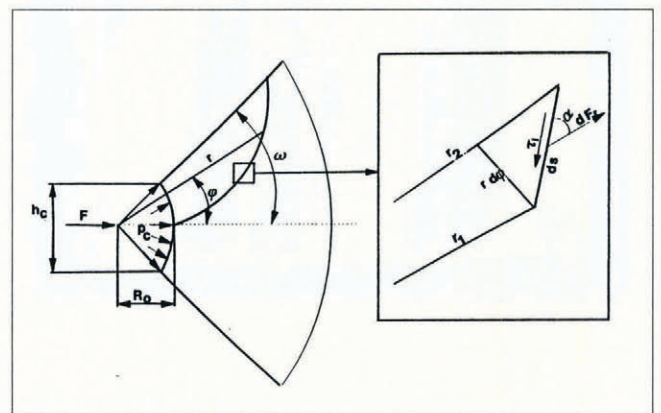


Fig. 4. Geometry of the wedge and flaking failure studied.

shaped ice edge with wedge angle of 2ω and unit breadth is considered, as shown in Figure 4.

It is assumed that the tip of the wedge is crushed so that the contact height is h_c and contact pressure is p_c causing a load $F = p_c h_c$ on the wedge. A radial stress state on the wedge in the plane stress condition is assumed as given below (Timoshenko and Goodier, 1970):

$$\sigma_r = \frac{2F \cos(\psi)}{r(2\omega + \sin(2\omega))}, \sigma_\psi = 0, \sigma_{r\psi} = 0 \quad (7)$$

where r and ψ are polar coordinates with origin at the tip of the wedge and σ_r is the radial compressive stress on the wedge.

Now the problem is to find a shape, $r = r(\psi)$, of the flaking failure surface, which minimises the force F required to cause the failure. The failure is assumed to initiate at the middle of the contact (axial splitting type of failure) and propagate following the slip surface, along which the ice is assumed to be in a failure state as determined by Equation (3). The stress components on a infinitesimal part of the slip surface having length ds , as shown in Figure 4, have to be in balance. The radial force acting on the surface ds is :

$$dF_r = \sigma_r r d\psi \quad (8)$$

and if the small surface length ds forms an angle α with the radial direction, the shear and normal stress components on the surface are:

$$\tau_s = \frac{dF_r \cos(\alpha)}{ds} = \frac{\sigma_r r \cos(\alpha) d\psi}{ds} \quad (9)$$

$$\sigma_s = \frac{dF_r \sin(\alpha)}{ds} = \frac{\sigma_r r \sin(\alpha) d\psi}{ds} \quad (10)$$

The relationship between ds and $d\psi$ can be obtained from simple geometry:

$$ds = \frac{rd\psi}{\sin(\alpha)} \quad (11)$$

Now, substituting Equations (9) and (10) in the Coulomb failure criterion (Equation (3)) and taking into account the relationship defined by Equation (11), the following function for the inner shear stress τ_1 is obtained:

$$\tau_1 = \sigma_r \sin(\alpha) (\cos(\alpha) - \sin(\alpha) \tan(\phi)) \quad (12)$$

The shear stress τ_1 is the shear carried by the material, after the shear carried by the friction due to the compressive stress is omitted from the total shear stress. The unknown direction angle α can be solved by minimising the force required for the failure. The minimum force is reached with angle α , which gives a maximum value for τ_1 :

$$\frac{d\tau_1}{d\alpha} = \frac{d}{d\alpha} (\sin(\alpha) \cos(\alpha) - \sin(\alpha)^2 \tan(\phi)) = 0 \quad (13)$$

By conducting the derivation of Equation (13) and using standard trigonometric transformations, it can be shown that the maximum value for τ_1 is achieved when:

$$\tan(2\alpha) = \frac{1}{\tan(\phi)} \quad (14)$$

This equation can also be presented in the form:

$$\tan(\alpha) = -\tan(\phi) + \sqrt{1 + \tan(\phi)^2} \quad (15)$$

According to Equation (15), the most probable shape of the slip surface is a curve, which has the character that the angle between curve's tangent and radial direction is constant and the change is only function of the internal friction angle of the material. The logarithmic spiral has this property the function for the curve being:

$$r = C_1 e^{C_2 \psi} \quad (16)$$

where C_2 is inversely proportional to $\tan(\alpha)$:

$$C_2 = \frac{1}{\tan(\alpha)} = \tan(\phi) + \sqrt{1 + \tan(\phi)^2} \quad (17)$$

C_1 is another constant and it can be solved from the initial condition describing the contact with a straight line; see Figure 4:

$$\psi = 0 : r = R_0 = \frac{h_c}{2 \tan(\omega)} \rightarrow C_1 = \frac{h_c}{2 \tan(\omega)} \quad (18)$$

Assuming that the shape of the slip surface follows the spiral defined by Equation (16), the next problem is to calculate the force required to reach the failure state along this curve. This can be obtained by integrating the function (12) with $\tau_1 = S_1$ along the slip surface. The integral takes the following form, taking into account also the stress state Equation (7), the relationship between ds and $d\psi$ from Equation (11) and rearranging the terms:

$$F = \frac{2\omega + \sin(2\omega)}{2\omega} S_1 C_1 \int_0^\omega \frac{1 + C_2^2}{(C_2 - \tan(\phi))} \cdot \frac{e^{C_2 \psi}}{\cos(\psi)} d\psi \quad (19)$$

In Equation (19) all the trigonometric functions including angle are represented as a function of C_2 using the relationship given by Equation (17). The integral cannot be solved in closed form and some numerical approach is needed.

Now the validity of formula (17) for determination of C_2 as a function of inner friction angle ϕ can be checked by minimising the integral (19) with respect to C_2 and comparing the results. This was done by varying the wedge angle ω and inner friction angle ϕ . The calculations proved that the following function for C_2 gives the minimum force:

$$C_2 = \tan\left(\phi - \frac{\omega}{3.1}\right) + \sqrt{1 + \tan\left(\phi - \frac{\omega}{3.1}\right)^2} \quad (20)$$

When comparing this result with Equation (17), it can be

concluded that Equation (17) is valid with small wedge angles, but with increasing wedge angles C_2 is decreasing, increasing the curvature of the spirals.

Comparison of the curved flaking theory with straight flaking theory

In this section the force required for failure along curved flakes or straight flakes is compared. The comparison is done by calculating the relation p_c/S_i required to cause the failure with various wedge angles and inner friction coefficients ϕ . Using $F = p_c h_c$ and calculating the value for C_1 with Equation (18), the integral (20) can be presented in the following form:

$$\frac{p_c}{S_i} = \frac{2\omega + \sin(2\omega)}{4\omega \tan(\omega)} \frac{1 + C_2^2}{C_2 - \tan(\phi)} \int_0^\omega \frac{e^{C_2\psi}}{\cos(\psi)} d\psi. \quad (21)$$

Similarly the criteria for flaking can be presented (Daley, 1991, p. 33):

$$\frac{p_c}{S_i} = 1/(\sin(\alpha) - \cos(\alpha) \tan(\phi)) \left(\cos(\alpha) - \frac{\sin(\alpha)}{\tan(\theta)} \right) \quad (22)$$

where $\alpha = \frac{\theta + \phi}{2}$, and $\theta = \frac{\pi}{2} - \omega$.

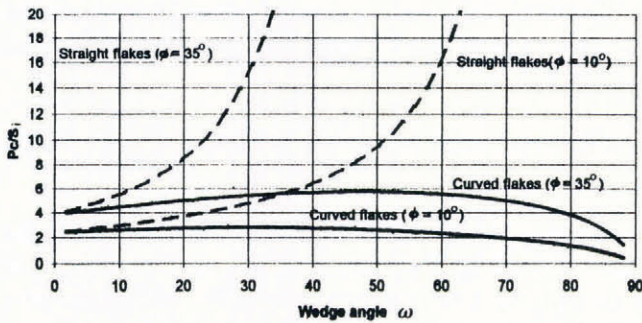


Fig. 5. Comparison of the p_c/S_i required for the spalling and flaking process as a function of the wedge angle and inner friction angle as a parameter.

The Equations (21) and (22) are plotted in Figure 5 as a function of the wedge angle and with two values for the inner friction angle ($\phi = 10^\circ$, $\phi = 35^\circ$). As can be seen, the curved flakes require much lower contact pressures than the straight flakes with bigger wedge angles. This difference is due to the more realistic stress distribution used when developing the criteria for curved flaking.

Application of the model to study the ice failure process

As stated above, failure process modelling is initiated by ice crushing at the contact, which continues until the crushing force is high enough to cause flaking failure according to Equation (19). Flaking failure can run into the upper or lower surface of the ice and also, after the first flaking failure, to the surface of the previous flake, which can be considered as second-order failure as shown in Figure 6. After the flaking failure the contact height is cut in half and the crushing continues until the next flaking failure takes place. The search for the shape of the flaking failure results in an iterative procedure as the angle of the ice edge, to which the spall runs, has also an effect on the shape according to Equation (20). The other

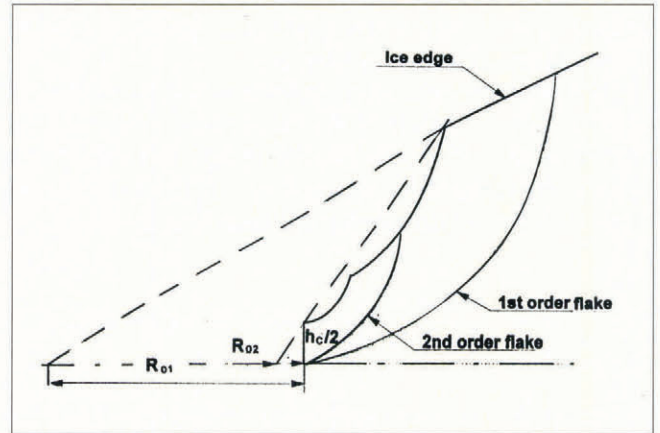


Fig. 6. Schematic presentation of the methods to determine the tip of the wedge.

shape parameter C_1 is determined using Equation (18), which specifies the location of the wedge tip. Figure 6 also illustrates the approach used to determine the tip of the wedge, which is determined based on the shape of the unbroken wedge for 1st order flakes (R_{01}) and on the shape of the 1st order flake for 2nd order flakes (R_{02}).

NUMERICAL EXAMPLES

The calculation model is compared with the force time history measured during test no. 76 of the laboratory crushing tests of Joensuu and Riska (1989). The wedge angle was 45° ($2\omega = 90^\circ$), ice thickness was 0.249 m, temperature of ice was -5°C and crushing speed was 50 mm s^{-1} . According to Daley (1991), the following numerical values can be used for ice mechanical properties:

$$\mu + 0.1, \quad \phi = 35^\circ, \quad S_c = 1.17 \text{ MPa}, \quad S_i = 643 \text{ kPa}.$$

As defined above a value of 38 MPa is used for the contact pressure p_c . Figure 7 gives the measured time history with a crushing speed of 50 mm s^{-1} together with the simulated time histories using straight flake theory (Daley, 1991) and the curve flake theory presented in this paper. First and second level flakes are used during the simulation.

As can be seen, the straight flake theory demands twice as high a load level as the curved flake theory. The curved flake model gives a load level close to the measured level. The time history with straight flake model given in this paper differs considerably from that given by Daley (1991), as he modifies the ice thickness due to the end-flaking of the test piece, which lowers load level and increases flaking frequency. This effect can also explain the somewhat higher level of simulated force than measured force with the curved flake model.

CONCLUSIONS

The curved flaking model developed includes the effect of radial stress distribution on compressive failure of a wedge-shaped ice edge. This gives rise to curved flakes in

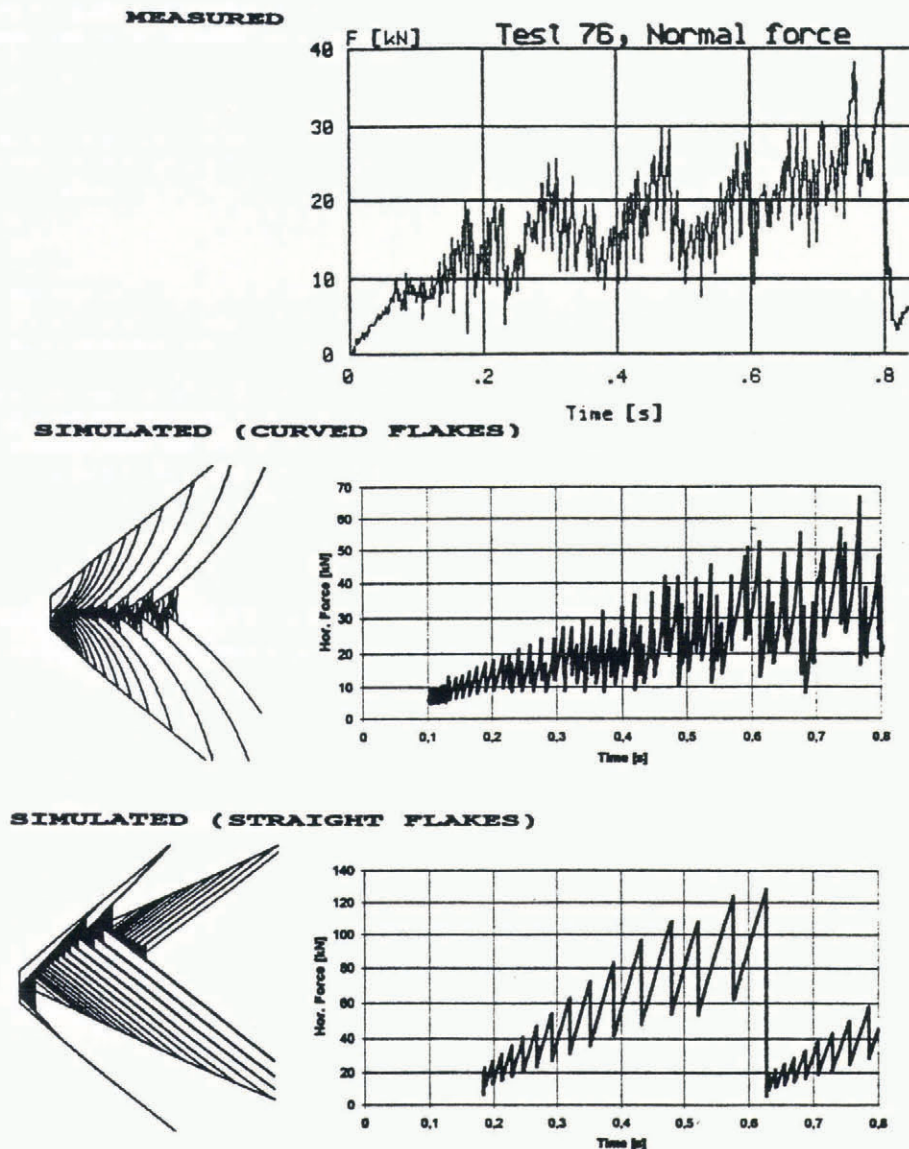


Fig. 7. Comparison of the measured and simulated crushing forces.

the shape of logarithmic spirals. Comparison of the force required for flaking using a straight or curved flaking model indicates considerably lower values for the force with curved flakes. This difference increases with increasing wedge angles. The model is used to simulate an ice-crushing test, in which a fairly good correspondence is obtained with simulated values somewhat above the measured values. This can be due to the effect of the possible end-flaking of the test pieces, which is not included in the study.

Curved flakes can have strong curvature, which indicates also that the failed ice can carry loads in the contact. The wider the wedge angle and the thicker the ice, the more pronounced the effect that can be predicted to be caused by ice extrusion. The distinction between the crushing zone and flaking failures therefore diminishes with small and steep flakes. This can give new insight to the modelling of the crushed zone.

Other important topics which are not covered in this paper are the effect of crystal orientation on the process and the possibilities of extending the model into the third dimension to study wide contacts and non-simultaneous failures.

ACKNOWLEDGEMENTS

Financial support from the Academy of Finland has made this study possible, and is here gratefully acknowledged.

REFERENCES

- Ashby, M.F. and S.D. Hallam. 1986. The failure of brittle solids containing small cracks under compressive stress states. *Acta Metallurgica et Materialia*, **34**(3), 497–510.
- Daley, C. 1991. Ice edge contact; a brittle failure process model. *Acta Polytech. Scand. Mech. Eng. Ser.*, **100**.
- Fransson, L., T. Olofsson and J. Sandkvist. 1991. Observations of the failure process in ice blocks crushed by a flat indenter. In Muggeridge, D.B., D.B. Colbourne and H.M. Muggeridge, eds. *POAC'91. The 11th International Conference on Port and Ocean Engineering under Arctic Conditions, September 24–28, 1991, St. John's, Canada. Volume I*. St. John's, Memorial University of Newfoundland, 501–514.
- Gagnon, R.E. and N.K. Sinha. 1991. Energy dissipation through melting in large scale indentation experiments on multi-year sea ice. In Ayorinde, O.A., N.K. Sinha, W.A. Nixon and D.S. Sodhi, eds. *Proceedings of the 10th International Conference on Offshore Mechanics and Arctic Engineering 1991. Volume IV. Arctic/polar technology*. New York, American Society of Mechanical Engineers, 157–161.
- Hallam, S.D. and J.P. Nadreau. 1988. Failure maps for ice. In Sackinger, W.M. and M.O. Jeffries, eds. *Port and Ocean Engineering*

- under Arctic Conditions. Volume III. Fairbanks, AK, University of Alaska. Geophysical Institute, 45–55.
- Hobbs, P. V. 1974. *Ice physics*. Oxford, Clarendon Press.
- Jaeger, J. C. and N. G. W. Cook. 1979. *Fundamentals of rock mechanics*. Third edition. London, Chapman and Hall.
- Joensuu, A. and K. Riska. 1989. *Contact between ice and a structure*. Otaniemi, Helsinki University of Technology. Laboratory of Naval Architecture and Marine Engineering. (M-88.) [In Finnish.]
- Kendall, K. 1978. Complexities of compression failure. *Proc. R. Soc. London., Ser. A.*, **361**, 245–262.
- Kujala, P., R. Goldstein, N. Osipenko and V. Danilenko. 1993. *A ship in compressive ice. Analysis of the ice failure process*. Otaniemi, Helsinki University of Technology. Faculty of Mechanical Engineering. Ship Laboratory. (M-165.)
- Nemat-Nasser, S. and H. Horii. 1982. Compression-induced nonplanar crack extension with application to splitting, exfoliation, and rockburst. *J. Geophys. Res.*, **87**(B8), 6805–6821.
- Riska, K., H. Rantala and A. Joensuu. 1990. *Full scale observations of ship-ice contact*. Otaniemi, Helsinki University of Technology. Faculty of Mechanical Engineering. Laboratory of Naval Architecture and Marine Engineering. (M-97.)
- Sanderson, T. J. O. 1988. *Ice mechanics; risks to offshore structures*. London, Graham and Trotman.
- Schulson, E. M. 1990. The brittle compressive fracture of ice. *Acta Metallurgica et Materialia*, **38**(10), 1963–1976.
- Schulson, E. M. and T. R. Smith. 1992. The brittle compressive failure of columnar ice under biaxial loading. In IAHR'92. *Proceedings of the 11th International Symposium on Ice 1992, Banff, Alberta. Volume 2*, 1047–1064.
- Timoshenko, S. P. and J. N. Goodier. 1970. *Theory of elasticity. Third edition*. Tokyo, MacGraw-Hill.
- Tuhkuri, J. 1993. *Laboratory tests of ship structures under ice loading. Volume 1*. Otaniemi, Helsinki University of Technology. Faculty of Mechanical Engineering. Ship Laboratory. (M-166.)
- Varsta, P. 1983. On the mechanics of ice load on ships in level ice in the Baltic Sea. *Technical Research Center of Finland. Publication 11*.
- Wierzbicki, T. 1985. Spalling and buckling of ice sheets. In Bennett, F. L. and J. L. Machemehi, eds. *Civil engineering in the Arctic offshore. Proceedings of the Conference Arctic '85, San Francisco, California, March 25–27, 1985*. New York, American Society of Civil Engineers, 953–961.
- Wierzbicki, T. and D. G. Karr. 1988. Structural imperfections and interactive failure of edge loaded ice sheets. In Sackinger, W. M. and M. O. Jeffries, eds. *Port and Ocean Engineering under Arctic Conditions. Volume III*. Fairbanks, AK, University of Alaska. Geophysical Institute, 369–380.

The accuracy of references in the text and in this list is the responsibility of the author, to whom queries should be addressed.